The Outcome of Therapeutic Trials using Iron and Iron Chelator in Acute Murine Toxoplasmosis: Histopathological and Immunohistochemical study

Eman M Abdel-Rahman[1], Basma H Abdel-Hameed[1], Asmaa M Yousef[1]

[1]*Medical Parasitology Department, Faculty of Medicine, Zagazig University, Zagazig, Egypt*

Corresponding Author
Asmaa M Yousef
Mobile:
+201023062767
Email:
drasmayousef@gmail.com

Receive date:25/2/2024
Revise date:17/4/2024
Accept date:19/5/2024
Publish date:25/5/2024
Keywords:
T. gondii; Iron; Deferoxamine; Immunohistochemical; IL-6; TGF-β.

Background and study aim: Iron has a critical part in several biological activities. Maintaining an optimal iron balance becomes especially important in the case of *Toxoplasma gondii.* This study aimed to assess the effects of iron and iron chelator, deferoxamine on toxoplasmosis outcome in the experimental mice utilizing histopathological and immuno-histochemical assessment of IL-6 and TGF- β levels expression in liver tissue.

Patients and Methods: Sixty Swiss albino male mice were divided up into four equal groups as follows: (GI): control negative non-infected non-treated group; (GII): control positive, infected non-treated group; (GIII): infected iron supplemented group; (GIV): infected deferoxamine treated group.

Results: Our data indicated that infected group (GII) showed marked histopathological changes represented by portal biliary reaction and lymphocytic cholangitis. The infected iron-supplemented group (GIII) exhibited marked histopathological changes of focal hepatocellular degeneration, scattered necrosis and apoptosis in liver tissues of experimentally infected mice that were greatly improved in GIV after chelation of iron using deferoxamine treatment. These findings were confirmed by immuno-histochemical assessment to investigate the expression of Il-6 which was highly expressed in GIII; 46.29 ± 13.89, but its expression was low in GIV; 10.49 ± 3.04 (p <0.001). Conversely, the highest expression of TGF-β was in GIV; 49.18 ± 12.3 and its expression was low in GIII; 12.45 ± 3.61 (p <0.001).

Conclusion: Our findings suggest that deferoxamine can be a promising treatment for acute *Toxoplasma (T.) gondii* infection due to the limited availability of iron.

INTRODUCTION

Toxoplasma gondii (T. gondii) is a common protozoan that is capable of causing serious illness in those with compromised immune systems [1]. *T. gondii* is considered one of the tops "Five Neglected Parasitic Infections" by the Centers for Disease Control (CDC) [2] because of its high incidence, the seriousness of its illness, and the possibility of prevention [3].

T. gondii is peculiar in that it can infect all types of nucleated cells seen in humans and warm blooded animals [4]. The parasite may infect any cell; therefore, it can damage other organs such as the heart [5], eyes [6], kidney [7], and liver [8]. Many investigations have found that the parasite produces a variety of pathological alterations in the liver, including hepatitis, granuloma hepatomegaly, and necrosis [8]. Furthermore, Ustun and coworkers demonstrated that *T. gondii* infection is related with hepatic cirrhosis [9]. Acute phase response is often triggered by inflammation, which may be localized near the organism. However, the systemic acute phase responses include endocrine, neurological and hepatic gene expression alterations [10].

The liver is a vital organ responsible for all aspects of metabolism, including the breakdown of carbohydrates, lipids, and proteins, as well as the detoxification of xenobiotic and drugs [11].

The drugs recommended for treating or preventing toxoplasmosis are sulfadiazine and pyrimethamine, but they possess severe adverse effects. Although there are alternative medications on hand, their tolerance is low [12]. Consequently, it is imperative to discover a new treatment that has the ability to inhibit the spread of T. gondii tachyzoites to other organs [13].

Iron plays a crucial role in different cellular processes, including oxygen transport, respiration, and DNA synthesis. Moreover, iron is essential for many vital biological functions such as heme biosynthesis [14], biogenesis of iron-sulphur clusters [15], and acting as a cofactor for a number of crucial proteins, including propyl hydroxylases [16] and catalase [17].

The hexadentate iron chelator deferoxamine (DFO) mesylate possesses antioxidant properties [18]. In cases of iron storage diseases, it is utilized as a chelator in clinical medicine to remove iron. Iron bound by DFO making it metabolically inactive, preventing or reversing free radical production's effects. Therefore, it reduces oxidative damage in vital organs and it may even lead to improved survival in vivo and in vitro studies [19].

Iron acquisition and utilization have been investigated in some pathogenic parasites, such as *Trichomonas* [20]. Additionally, they have been extensively studied in blood flagellates, like *Leishmania* [21] and *Trypanosoma* [22]. Interleukin 6 (IL-6) is the main mediator responsible for hepatocytic production of acute inflammatory phase proteins. Further, in murine toxoplasmosis, a gradual increase in serum IL-6 is correlated with clinical signs [23]. Transforming growth factor-β (TGF-β) is well-known for its immunosuppressant action. Also, the anti-inflammatory action of this cytokine makes it possible to control the development of immunopathological phenomena related to a type-1 immune response [24]. Yet research on iron use in toxoplasma is still lacking. Therefore, the present study aims to evaluate the effect of adding or removing iron on the outcome of T. gondii infection in the liver of mice using histopathological and Immunohistochemical analysis of IL-6 and TGF- β expression.

PATIENTS/MATERIALS AND METHODS

"The avirulent (Me49) strain of *T. gondii*:"

This experimental study was conducted from July 2023 to December 2023 at the Parasitology Department, Faculty of Medicine, Zagazig University in Egypt. Me49 type II cystogenic Toxoplasma strain was generously obtained from the Medical Parasitology Department, Faculty of Medicine, Alexandria University. Using a 22-gauge blunt feeding needle and a quantity of brain homogenate calibrated to produce 10 tissue cysts to retain the survival rate of mice. The strain was maintained by oral passage as it is the most naturalistic route of infection in outbred Swiss albino mice through administering cysts per mouse orally; the cysts were obtained from brain homogenate of mice that had been infected with the Me49 strain of *T. gondii* for at least eight weeks. Tissue cysts were counted in 10 µL of the brain suspension using light microscopy [25].

Experimental animals

Sample size was calculated to be not less than 40. The sample size was calculated using the Open Epi program with a confidence level of 95% and power of 80%.

In our experiment, sixty Swiss albino male mice were free of parasites that were 3-4 weeks old and weighed 20-25 grams. The mice were kept in well-ventilated cages and could accommodate 20 mice per cage. The bedding was changed daily to ensure a clean environment for the mice. The animals were provided with conventional pelleted food and had unrestricted access to water. They were kept in compliance with the research protocols following the recommendations of the National Institutes of Health Guidelines for the Use of Animals in Research.

Experimental design

Sixty mice were classified into four groups; 15 mice each **(GI):** Control negative non-infected non-treated group. (**GII):** Control positive Infected non-treated group injected intraperitoneally (I.P) with vehicle (phosphate buffered saline) (PBS) the day before infection and for seven more days following infection. **(GIII):** Infected iron sucrose-treated group**.**

(GIV): Infected deferoxamine (DFO)-treated group.

Drugs

(Iron sucrose) iron saccharate ($C_{12}H_{29}Fe_5Na_2O_{23}$): Scrofer, manufactured and provided by Amoun Pharmaceutical Company, Egypt. The dosage chosen for the current work was therapeutic dose to treat the iron deficiency anaemia of 80mg/kg/ day [26]. **Deferoxamine mesylate** ($C_{26}H_{52}N_6O_{11}S$)**:** Desferal, provided by Novartis, Egypt. The chosen dosage for this study was 300mg/kg/day [27]. Both drugs were administered intraperitoneally one day prior to infection and for a further seven days following infection, according to the drug table of Paget and Barnes [28]. Assessment during acute stage after completing the treatment. all animals were euthanized by cervical dislocation following the last dose of therapy. Hepatic tissue was taken for doing the following assessments.

I. Histopathological assessment:

Haematoxylin and eosin staining

After fixing in 10% formalin for 24 hours, samples were rinsed for twelve hours in water and dried in progressively increasing ethanol concentrations (120 minutes at 70% ethanol, 90 minutes at 90% ethanol, and one hour at 100% ethanol (two cycles). Following a one-hour immersion in a 50% ethanol and 50% xylene combination, the samples were cleaned for a further 1.5 hours in pure xylene. The samples were then covered with paraffin wax. The paraffin slices (4–5 µm) were stained with Haematoxylin and eosin [29]. The degree of inflammatory cell infiltration in the hepatic tissue was assessed. Five histological sections were examined in each mouse. Then, ten low-power fields (100×) from each of the examined sections were determined to calculate the average score (A mild reaction is denoted by +1, a moderate reaction by +2, and an extreme reaction by +3) [30].

Iron Staining of the infected mice's liver:

The assessment of iron accumulation in the liver was conducted using Perl's staining. Sections that had been deparaffinized were first immersed in a solution containing 10% potassium ferrocyanide for five minutes at room temperature (Merck KGaA, Darmstadt, Germany). They were incubated for twenty minutes in a solution containing hydrochloric acid 10% (Merck S.A., Rio de Janeiro, RJ, Brazil). To counterstain the slides, nuclear fast red was used (Merck KGaA, Darmstadt, Germany) and then examined using a 40× objective by light microscopy [31].

Congo red staining

Some paraffin-embedded tissue sections of GIII were stained with Congo red stain for detection of amyloidosis because iron overload accelerates the production of amyloid β. We prepared the stock solution as the following: Congo red 0.2% solution: Add the Congo red dye (0.1 g) (cat. no. C6767, Sigma-Aldrich) to 500 ml of saturated NaCl solution, making sure to leave a layer of NaCl at the bottom. Before using, let the mixture stir for a whole night. A dark glass bottle will keep the solution fresh for a very long period. Filtration is required before using this solution [32].

II. Immunohistochemical assessment:

Immunohistochemical study was carried out to investigate the expression of IL-6 and TGF- β levels. Liver sections were embedded in paraffin after being fixed in formalin 10%, after that, the sections were mounted on glass slides with a positive charge (Biogenex, USA). Expression of IL-6 and TGF-β levels were evaluated using the biotin-peroxidase-ABC method. The slices were incubated in phosphate-buffered saline (PBS) for five minutes; the sections were submerged in citrate buffer solution (pH 6) in a microwave for twenty minutes to facilitate antigen retrieval. An endogenous peroxidase-blocking reagent containing sodium azide and hydrogen peroxide was incubated with tissue sections (DAKO, Cat. No. S2001) in compliance with the guidelines suggested by the manufacturer. After rinsing, tissue sections were incubated with primary monoclonal antibodies against both IL-6 (Cat. No. 406-ML-005) and TGF-β (Cat. No. NBP2-11921B) (Novus Biologicals, LLC, USA). Next, the avidin-biotin-peroxidase complex was incubated in each section. (ABC kit, PK-4000). 3, 5 diaminobenzidines (DAB) substrate was used for visualization (DAKO Corp, Fremont, CA, USA). y. These sections were inspected with a light microscope (Olympus, Hamburg, Germany) using a grading scale: 0=no cells, 1=few cells (low densities), 2=many cells (high densities) [29].

IL-6 and TGF-b1 immuno-activity quantitation

was made by digital image analysis through the image J analysis software on five fields from each slide. This software could measure the total positive stained brown color/areas throughout the unstained cells. From this data an index (positively stained cells per a total of 1000 cells) can be computed (JID801D).

Statistical analysis

The collected data were computerized and statistically analyzed using the Statistical Package for Social Sciences SPSS program version **27.0**. Quantitative data were expressed as mean ± SD (Standard deviation). ANOVA test was used to calculate the difference between quantitative variables in more than two groups in normally distributed data. Image J software analytical estimation was used. Statistical comparisons were done with significance Level of P-value ≤ 0.05 indicates significant, p <0.001 indicates a highly significant difference while P> 0.05 indicates a non-significant difference.

RESULTS

Mice death during the experimental study: There was no significant difference in the survival and mortality rates among the different studied groups as we started our experiment with 45 infected mice, and 15 mice as negative control. By the end of the experiment, 8 infected mice, and 2 control mice had died, while 37 and 13 mice, respectively survived till scarification. Survival rate in the infected and negative control group was 82.2% and 86.6% respectively. While the mortality among the studied groups rate was 17.7% and 13.3% respectively

I. Histopathological Results

Haematoxylin and Eosin stain:

Group I (non-infected control group):

Normal hexagonal hepatocyte plates were visible in serial sections obtained from the liver of this group. The hepatocytes are large and polyhedral cells. They may contain about two and four nuclei. The perisinusoidal space (also known as the space of Disse) is generated when the hepatocytes expand the villi into the perisinusoidal vascular space. Satellite cells inhabit space of Disse. There were no discernible signs of necrotic, apoptotic, degenerative, or inflammatory alterations **(Fig.1a).**

Group II (*T. gondii* Infected group):

Examined sections from liver of this group pointed out marked histopathological changes represented by portal biliary reaction, lymphocytic cholangitis, lymphoplasmacytic infiltration and interstitial aggregations with associated focal hepato-cellular necrosis and individual cells apoptosis. The most prominent feature was reticulo-endothelial cells proliferation. Some of the proliferating cells mostly arise from hepatic satellite cells (HSCs). These characteristic cells appeared as large, rounded, apple-shaped or atypically formed with intracellular nuclear proliferative activities and abundant eosinophilic cytoplasm **(Fig.1b).**

Group III (Iron-treated group):

Characteristic hepatic lesions were represented by marked portal and interstitial round cells aggregations, focal hepatocellular degeneration, scattered necrosis and apoptosis. Von-Kupffer cells proliferation, hypertrophic changes and focal endotheliosis. Also, Hepatic satellite cells with metamorphic and nuclear reactive changes were observed. Moreover, Focal and diffuse, per-arteriolar and subendothelial deposition of homogenous eosinophilic amorphous structureless materials were detected **(Fig.1c).**

Group IV (Deferoxamine -treated group)

Examined sections from liver of this group declared a less significant micromorphological lesions compared with the infected group as the changes were represented by mild to moderate hepatocellular degenerative changes with a few scattered necrotic and apoptotic cells. Mild portal lymphocytic infiltration, Von-Kupffer cells hyper reactive changes and transformation of some hepatic satellite stem cells to large typical and atypical metamorphic cells were recorded **(Fig.1d).**

Iron staining in the liver of infected mice:

The characteristic iron deposition (hemosiderin granules) was demonstrated in the cytoplasm of some hepatocytes, vascular endothelial cells, Von-Kupffer cells and macrophages. Stained hemosiderin particles were amorphous basophilic structures of variable shapes and sizes. The staining reactivity was noticeable in iron supplemented-Infected group (GIII) **(Fig.2c),** meanwhile, most of the examined sections of

groups I, II and IV were negatively stained **(Fig.2a, b, d).**

Congo red stain:

Amyloid deposition was markedly demonstrated in group III with presence of homogenous eosinophilic structureless materials, mostly sub endothelially between hepatocytes and portal-peri-arteriolar, in H&E stained sections. Such materials were specifically stained as magenta red materials in the same locations using Congo red stain **(Fig.3)**.

II. Immunohistochemical Results:

A. Interleukin 6 (IL-6):

Expressions of IL-6 have been identified as a reactive cytoplasmic brownish protein in some of the hepatic endothelial and Von-Kupffer cells. The hepatic tissues of the control free group (GI) exhibited a negative reaction. Moreover, almost identical reactivity was observed in the hepatic tissues of the group treated with deferoxamine (GIV) and seemed to be clear within the endothelial cells associated with amyloid deposition. Moderate to strong brownish cytoplasmic reactivity was pronounced in some hepatocytes, the hepatic peri-portal and para-portal inflammatory cells, vascular endothelial and activated Von-Kupffer cells. Such reactivity was detected in *T.gondii* infected control group (GII) and in the iron-supplemented infected group (GIII) which appeared with a comparable more potent immune reactivity **(Fig. 4).**

B. Transforming growth factor beta (TGF-β):

Immuno-reactivates of TGF-β signal were represented by mild brownish immunostaining of the Von-Kupffer cells of the liver in the non-infected control group (GI). On the contrary, the immunoreactive staining reaction was notable in *T.gondii* infected group (GII) where some of hepatic Von-Kupffer and vascular endothelial cells beside some of the centro-lobular and paracentral hepatocytes showed moderate brownish cytoplasmic stainability to the used marker. Immune reactivity of TGF-β in the infected-iron-supplemented group (GIII) denoted mild reactions in most of the examined hepatic cells, a part of some mildly stained hepatic Von-Kupffer cells. DFO treated group (GIV) demonstrated a strong number of reactive hepatocytes, reticulo-endothelial cells. Positive cells showed marked brownish cytoplasmic stainability to the used marker (Fig.5).

Morphometric Findings:

Image J soft wear analytic estimation of immune- reactive cells of IL-6 and TGF-β in the different studied groups were recorded. Hepatic control free group (GI) denoted the estimated percentages of positivities of IL-6 and TGFβ as 6.61 ± 1.59 and 1.22 ± 0.27 respectively in the liver tissues. Meanwhile in control-infected group (GII), the percentages of positivities of IL-6 and TGFβ were 39.54 ± 8.7 and 32.94 ± 9.88 in the liver tissues. Also in infected-iron supplemented group (GIII), the percentages of IL-6 and TGFβ were 46.29 ± 13.89 and 12.45 ± 3.61 in the liver tissues. Infected-DFO supplemented group (GIV) showed the percentages of IL-6 and TGFβ as 10.49 ± 3.04 and 49.18 ± 12.3 respectively in the liver tissues [Table 1].

DOI: 10.21608/AEJI.2024.272563.1360

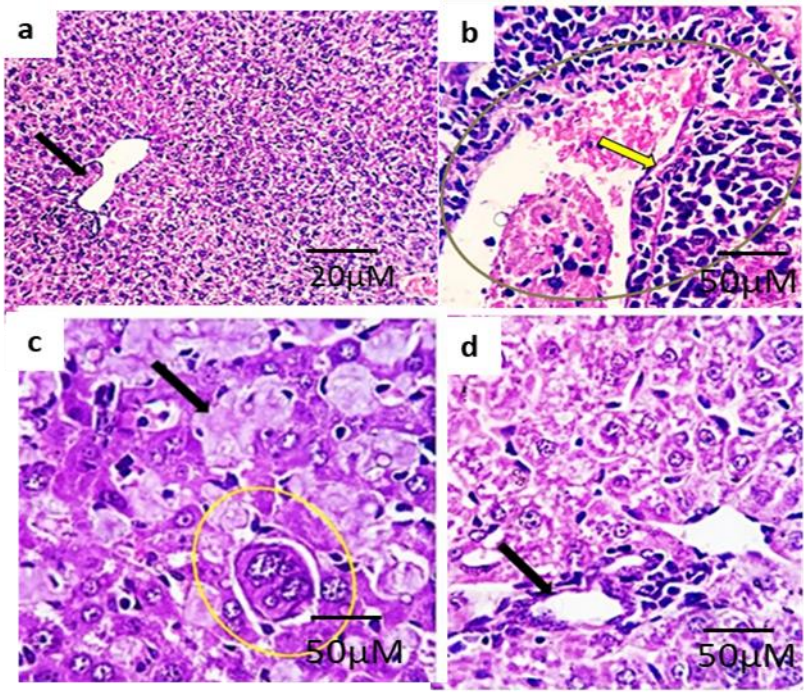

Figure 1. Fig 1: Photomicrographs of a section in the liver from non-infected control group (GI) showed apparently normal hepatic parenchymal with preserved central veins (black arrows) (Fig.1a ×100). Photomicrographs of a section from infected control group (GII) showed portal biliary reaction, lymphocytic cholangitis perivascular aggregations with associated focal hepato-cellular necrosis and individual cells apoptosis (yellow arrow, grey circle),(Fig.1b×400). Photomicrographs of a section from iron supplemented-infected group (GIII) showed portal and interstitial round cells aggregations, focal hepatocellular degeneration, Von -Kupffer cells hypertrophic changes, focal endotheliosis and amyloid deposition (black arrow). Hepatic satellite cells also seen (yellow circle) (fig.1c ×400). Photomicrographs of a section from Deferoxamine-treated group (GIV) showed mild to moderate hepatocellular degenerative changes with a few scattered necrotic and apoptotic cells. Mild portal lymphocytic infiltration (black arrow) (Fig.1d ×400) H&E.

Table 1: Comparison between the percentage of positivity of IL-6 and TGF-β in the liver tissues in the different studied groups

Group	IL-6 (Mean ± SD)	TGF-β (Mean ± SD)
GI (control -ve)	6.61 ± 1.59	1.22 ± 0.27
GII (control +ve)	39.54 ± 8.7	32.94 ± 9.88
GIII (iron treated)	46.29 ± 13.89	12.45 ± 3.61
GIV (DFO treated)	10.49 ± 3.04	49.18 ± 12.3
F	51.839	62.575
P	<0.001*	<0.001*

SD: Standard deviation F: ANOVA test *: highly significant (P<0.001)

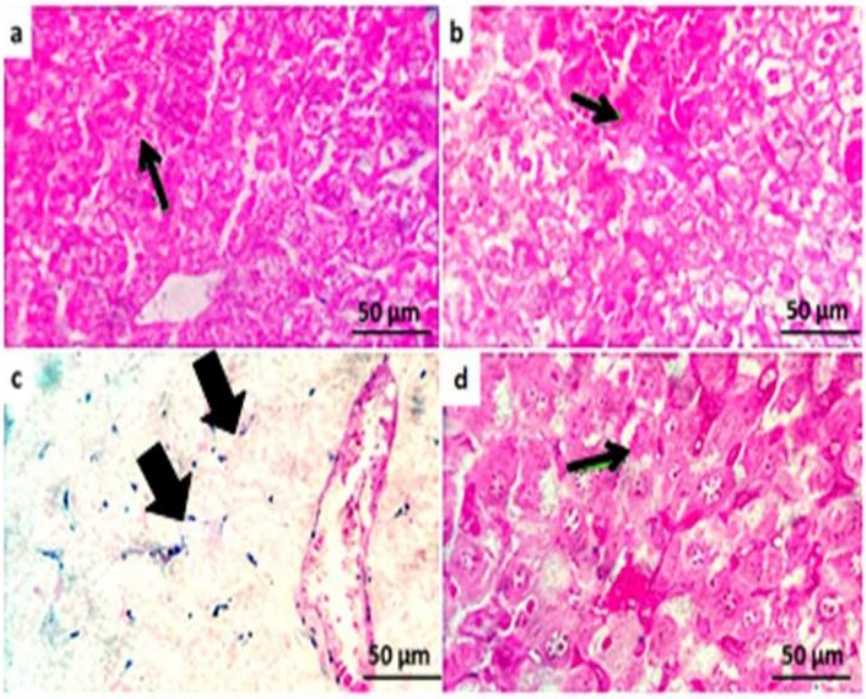

Figure 2. Photomicrographs from liver of different experimental sections showing positive iron deposition (hemosiderin granules) (broad black arrows) in the cytoplasm of some hepatocytes, vascular endothelial cells, Von-Kupffer cells and macrophages of GIII. Most of the examined sections of groups I, II and IV were negatively stained (thin black arrows) (Perl's stain ×400).

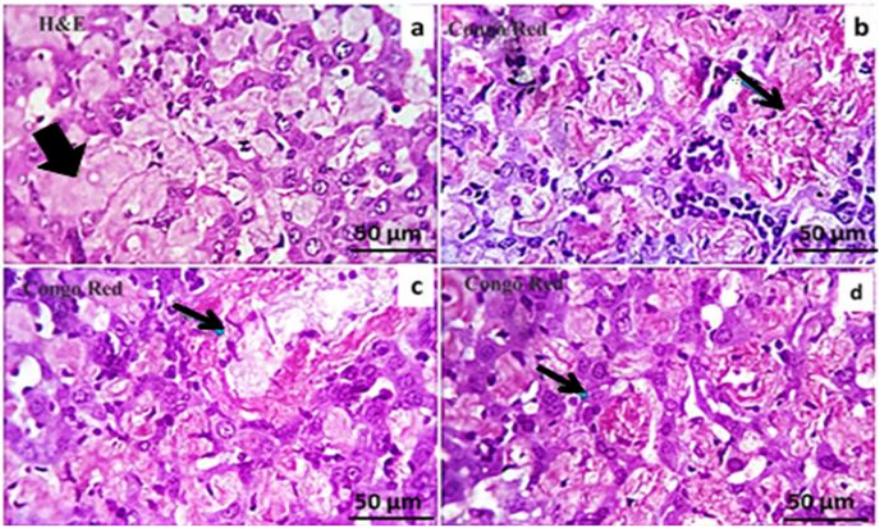

Figure 3. Photomicrograph from liver of infected–iron supplemented group (GIII) showed subendothelial and peri-arteriolar deposition of homogenous eosinophilic structureless materials, (H&E, broad black arrow). It appears as magenta red structures by Congo red stain (thin black arrows) ×400.

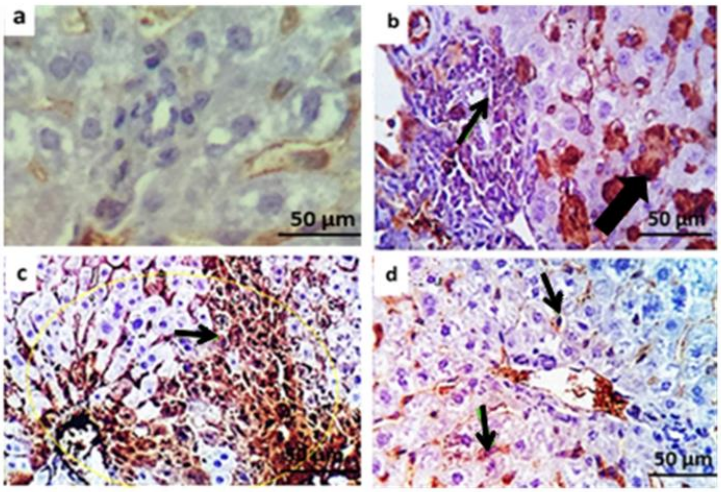

Figure 4. Photomicrographs of the liver tissues demonstrated their cytoplasmic reactivity against IL-6 in the various experimental groups. a: GI showing very mild expression in non-infected control group (×400). b: GII showing moderate expression in infected-control group (×400). c: GIII showing strong expression in iron supplemented-infected group (×400). d: GIV showing mild expression in DFO treated group (×400) (thin, broad black arrows).

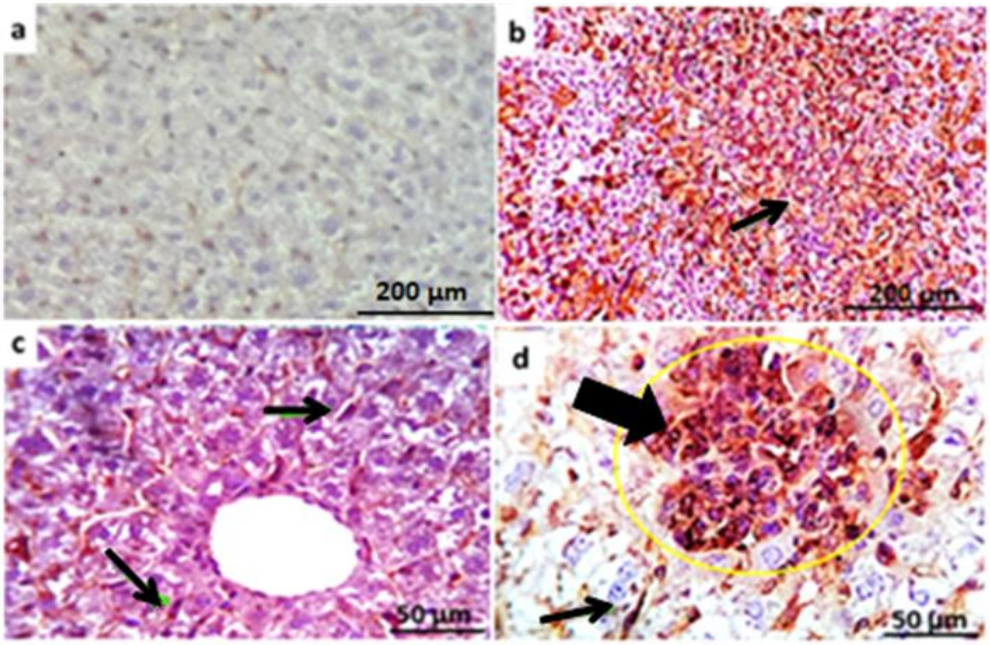

Figure 5. Photomicrographs exhibited hepatic tissues' cytoplasmic reactivity against TGF-β within each of the experimental groups (yellow circles, thin and broad black arrows). a: GI showing very mild expression in un infected control group (×200). b: GII showing moderate expression in T.gondii infected control group (×200). c: GIII showing mild expression in iron supplemented-infected group (×400). d: GIV showing strong expression in DFO treated group (×400).

DISCUSSION

T. gondii is important because it may avoid the immune system after an acute infection, causing a developmental transformation from rapid replicating tachyzoite to slow replicating latent bradyzoite in the brain. This shift from one parasite stage to the next produces chronic

infection. [33]. In this study, we concentrated on the acute stage of infection before transformation of bradyzoite in brain

The liver is an organ that stores excess bodily iron, thus it may play a crucial role in the parasite's development when iron supplements are taken [34]. Iron has a role in numerous biological reactions for instance, proteins essential to nucleic acid synthesis. From unicellular organisms to humans, all forms of life have evolved to retain these functions [35]. During infection whenever microorganisms and humans interact, the shared requirement for iron forms these interactions [36]. Further, iron is essential for metabolism, but because of its potential toxicity, storage and transportation must be carefully controlled [37]

In our study, several pathological changes were demonstrated in experimentally infected mice with *T. gondii* infection. In GII, the pathological changes in the liver tissues of mice were in the form of lymphocytic cholangitis, individual cells apoptosis, reticulo-endothelial cells proliferation with the multi-focal nodular formation compared to negative control group **(Fig.1a).** This observation is harmonious with He et al. and Alvarado-Esquivel et al. [38, 39] who found that acute *T.gondii* infection in the liver is associated with lymphocytic infiltration and apoptosis. The mechanisms underlying *T. gondii* infection-induced liver damage and histological alterations may be related to the parasite's direct proliferative effect on the tissues, which results in tissue damage and cell death, or they may be attributed to the indirect effect of the infection, which is caused by an overreaction by the immune system to the parasite. Moreover, in GIII, pathological changes in liver sections showed higher degree of inflammatory infiltration compared to GII **(Fig.1b,c).** It was reported that infected-iron supplemented group is associated with more inflammatory reactions when compared with other groups [27]. According to Dziadek et al. [40] *T. gondii* requires iron in order to survive and proliferate within its host cells. In addition, different studies suggested the availability of particular human lactoferrin-binding parasite receptors that contribute to the supply of host iron to the tachyzoites [41].

As regard, DFO-treated mice (GIV), inflammatory and degenerative changes were significantly lower in the liver samples when compared to infected control group (GII) **(Fig.1d)**. The results of Olivera et al. [27] who mentioned that DFO is associated with decreasing inflammatory score in experimentally infected mice with *T. gondii* corroborate these conclusions.

Interestingly, Dimier and Bout [42] stated that using the iron chelator, deferoxamine, inhibited the growth of the parasite intracellularly by limiting the availability of iron, a condition that was reserved by adding holotransferrin, an iron-saturated transferrin. Also, Almeida et al. [43] found that the DFO treatment had no impact on the cell viability suggesting that the reduction in iron availability to the parasite was what controlled the growth of *T. gondii*.

Moreover, Amyloid deposition was markedly demonstrated in GIII with presence of homogenous eosinophilic structureless materials, mostly sub-endothelial between hepatocytes and portal-peri-arteriolar, in H&E and congo red stained section **(Fig.1&3)**. This was in line with Atmaca and Atmaca [10] who demonstrated that *T.gondii* infected mice exhibited a statistically significant progressively rise in serum amyloid A levels on the 2nd, 4th, and 6th days post infection. Also, Becerril-Ortega et al. [44] explained that iron overload accelerates the production of amyloid β and results in cognitive impairment in transgenic mice and associated with many degenerative diseases such as alzheimer's disease. Researchers found that Amyloid peptide protein accelerates iron export by fixing the iron export protein, ferroportin, on the cell surface in a functional region [45]. Actually, multiple investigations have demonstrated that iron might increase the oxidative damage associated with Amyloid peptide aggregation [46].

In the current study, there was a notable expression of IL-6 in the liver tissues of mice (39.54 ± 8.7) in GII **(Fig.4).** Additionally, it was shown that BeWo trophoblasts and human monocyte cell lineage THP-1 cells, raised IL-6 levels in reaction to infection with *T. gondii* [43].

Moreover, clinical symptoms of murine toxoplasmosis are associated with a progressive increase in serum IL-6 [36]. It seems that IL-6 enhances *T. gondii's* intracellular growth in mice [47].

After iron saccharate supplementation, expression of IL-6 significantly increased in liver tissues of mice (46.29 ± 13.89) in GIII **(Fig.4)**. This observation is in an agreement with Olivera et al. [27] who stated that the infection raised IL-6 levels in the serum samples of both the infected group and the infected treated with iron.

IL-6 can regulate iron systemically via the induction of hepcidin hormone, which controls the iron entry to the bloodstream and imprisons it inside the enterocytes [48]. So, IL-6 needs to be adjusted since high IL-6 levels brought on by an oral *T. gondii* infection may promote the growth of the parasite, since the hepcidin-IL-6 axis makes iron more available inside the enterocytes, allowing the parasite to thrive [49].

As regards GIV (deferoxamine treated group), decrease of IL-6 expression (10.49 ± 3.04) in the liver sections of mice was detected **(Fig.4)**. This finding was in line with Aghabi et al. [37] who exhibited decrease inflammation and subsequently increase parasite survival after chelation of iron with deferoxamine. Furthermore, compared to infected control mice, deferoxamine therapy reduced IL-6 serum levels 1.65-fold, as demonstrated by Olivera et al. [27].

In this study, we found that TGF-β expression was elevated in liver sections (49.18 ± 12.3) in GIV compared to GII **(Fig.5).** These results coincide with the research conducted by Misumi et al. [50] who noticed that in rats infected experimentally, DFO is linked to increased TGF-β expression. Furthermore**,** Qayoom et al. [51] noted that deferoxamine was linked to increased TGF-β expression and was crucial in limiting infection, particularly in rats that were infected experimentally. In the same side, we demonstrated that increased expression of TGF-β in intestinal tissues was noticed when iron deprivation occurred [52].

Keep in mind that this cytokine stimulates regulatory T cells to modulate the immunological response. Overproduction and/or activation of TGF-β can influence the growth, migration, invasion, and survival of cells. Thus, a wide range of pathological conditions as tissue renewal result in increased TGF-β expression levels [53].

In conclusion: The present work showed that hepatic lesions in GIII were represented by focal hepatocellular degeneration, scattered necrosis and apoptosis. Examined sections from liver of GIV declared a mild hepatocellular degenerative changes with a few scattered necrotic and apoptotic cells. Chelation of iron using deferoxamine treatment showed histopathological improvement in liver tissues of experimentally infected mice with T. gondii parasite. These findings were confirmed by immunohistochemical assessment. Therefore, deferoxamine might be a hopeful drug to control acute T. gondii infection due to the limitation of iron availability. Iron supplementation in pregnant women can be beneficial for embryo/fetus development, but it can also promote parasite growth, increasing the chance of congenital infection. This paper lays the groundwork for future research on iron in T. gondii, which still has a lot of unanswered concerns.

Funding: None. Author funded

Conflict of Interest: None.

Ethical approval:

Permission and official approval to carry out the study was obtained. The ethical committee at the Faculty of Medicine, Zagazig University approved the experimental protocol. Approval number: ZU-IACUC/3/F/449/2023

Author contribution

We declare that the idea and design of the research were contributed to by all writers. All listed authors have made substantial contributions to the material preparation, the data collecting and analysis and writing the manuscript's initial draft. The final manuscript was read and approved by all writers.

Availability of data and materials:

The datasets used and/or analysed during the current study are available from the corresponding author on reasonable request.

HIGHLIGHTS

- Toxoplasmosis cause severe diseases in both animals and humans.
- It is imperative to discover new treatment to overcome drug tolerance and resistance

- Iron plays a crucial role in the different cellular processes and the vital biological functions of the parasite
- The iron chelator, deferoxamine, could be a promising drug to control acute *T. gondii* infection due to the limitation of iron availability.

REFERENCES

1. Pamukcu S, Cerutti A, Bordat Y, Hem S, Rofidal V, Besteiro S . Differential contribution of two organelles of endosymbiotic origin to iron-sulfur cluster synthesis and overall fitness in Toxoplasma. *PLoS Pathog*. 2021; 17(11): e1010096.
2. Molan A, Nosaka K, Wang W, Hunter M. Global status of *Toxoplasma gondii* infection. Systematic review and prevalence snapshots. *Tropical Biomedicine*. 2019; 36: 898–925.
3. Centers for Disease Control and Prevention. Parasites-Toxoplasmosis (Toxoplasma Infection): *Epidemiology and Risk* 2021. Available at https://www.cdc.gov/parasites/toxoplasmosis/epi.html.
4. Tarannum T, Alam MS, Rahman A, Chakraborty S, Shekhar HU, Rahman T. Analysis of Proteotranscriptomics Landscape Reveals Differentially Regulated Pathways in Toxoplasma gondii Infected Mouse Liver. Computational Molecular Bioscience. 2022 ; 4;12(1):20-57.
5. Manlio, et al. (2008) Temporal and Spatial Distribution of Toxoplasma gondii Differentiation into Bradyzoites and Tissue Cyst Formation in Vivo. Infection and Immunity, 76, 3491-3501. https://doi.org/10.1128/IAI.00254-08
6. Kadarisman, R.S., Marsetio, M. and Simangunsong, L.B. (1991) Visual Impairment and Blindness in Ocular. The Southeast Asian Journal of Tropical Medicine and Public Health, 9, 99-101.
7. Khurana, S. and Batra, N. (2016) Toxoplasmosis in Organ Transplant Recipients: Evaluation, Implication, and Prevention. Tropical Parasitology, 6, 123-128. https://doi.org/10.4103/2229-5070.190814
8. Alvarado-Esquivel, C., Torres-Berumen, J.L., Estrada-Martínez, S., Liesenfeld, O. and Mercado-Suarez, M.F. (2011) Toxoplasma gondii Infection and Liver Disease: A Case-Control Study in a Northern Mexican Population. Parasites & Vectors, 4, 75. https://doi.org/10.1186/1756-3305-4-75
9. Ustun, S., Aksoy, U., Dagci, H. and Ersoz, G. (2004) Incidence of Toxoplasmosis in Patients with Cirrhosis. World Journal of Gastroenterology, 10, 452-454. https://doi.org/10.3748/wjg.v10.i3.452
10. Atmaca N, Atmaca HT. The correlation of TNF alpha levels with acute phase proteins in acute Toxoplasma gondii infection in mice. *Experimental Parasitology*. 2022; 108311.
11. Alamri ZZ. The role of liver in metabolism: an updated review with physiological emphasis. *International Journal of Basic and Clinical Pharmacology*. 2018; 7 (11): 2271-2276.
12. Shammaa AM, Powell TG, Benmerzouga I. Adverse Outcomes Associated With the Treatment of Toxoplasma Infections. *Sci Rep*. 2021; 11 (1):1–8.
13. Black MW, Boothroyd JC. Lytic Cycle of Toxoplasma Gondii. Microbiol. *Mol Biol Rev*. 2000; 64 (3): 607–623.
14. Bergmann A, Floyd K, Key M, Dameron C, Rees KC, Thornton LB, et al. Toxoplasma gondii requires its plant-like heme biosynthesis pathway for infection. *PLoS Pathog. 2020;* 16(5): e1008499.
15. Aw YTV, Seidi A, Hayward JA, Lee J, Makota FV, Rug M, Dooren GG. A key cytosolic iron–sulfur cluster synthesis protein localizes to the mitochondrion of Toxoplasma gondii. *Mol Microbiol*. 2021; 115: 968–985.
16. Florimond C, Cordonnier C, Taujale R, van der Wel H, Kannan N, West CM, Blader IJ. A toxoplasma prolyl hydroxylase mediates oxygen stress responses by regulating translation elongation. *mBio*. 2019; 10: e00234–19.
17. Kwok LY, Schlüter D, Clayton C, Soldati D. The antioxidant systems in Toxoplasma gondii and the role of cytosolic catalase in defence against oxidative injury. *Mol. Microbiol*. 2004; 51: 47–61.
18. Kloehn J, Harding CR, Soldati-Favre D. Supply and demand— heme synthesis, salvage and utilization by Apicomplexa. *FEBS J*. 2021; 288: 382–404.

19. Rachidi S, Coudray C, Baret P, Gelon G, Pierre JL, Favier A. Inhibition of Lipid peroxidation by a new family of iron chelators. Comparison with desferrioxamine. *Biol Trace Elem Res.* 1994; 41: 77–87.

20. Sehgal R, Goyal K, Sehgal A. Trichomoniasis and lactoferrin: *future prospects. Infectious diseases in obstetrics and gynecology.* 2012; 2012: 536037.

21. Zaidi A, Singh KP, Ali V. Leishmania and its quest for iron: An update and overview. *Molecular and biochemical parasitology*. 2017; 211: 15-25.

22. Gilabert Carbajo C, Cornell LJ, Madbouly Y, Lai Z, Yates PA, Tinti M, Tiengwe C. Novel aspects of iron homeostasis in pathogenic bloodstream form Trypanosoma brucei. *PLoS pathogens.* 2021; 17(6):e1009696.

23. Filisetti D, Candolfi E. Immune response to Toxoplasma gondii. Ann Ist Super Sanita. 2004 Jan 1;40(1):71-80.

24. Buzoni-Gatel D, Debbabi H, Mennechet FJ, Martin V, Lepage AC, Schwartzman JD, Kasper LH. Murine ileitis after intracellular parasite infection is controlled by TGF-betaproducing intraepithelial lymphocytes. Gastroenterology 2001;120(4):914-24

25. Fuentes-Castro BE, Reyes-García JG, Valenzuela-Vargas MT, Martínez-Gómez F. Histopathology of murine toxoplasmosis under treatment with dialyzable leukocyte extract. *Mem Inst Oswaldo Cruz.* 2017; 112 (11): 741-747.

26. Kuo KL, Hung SC, Lee TS, Tarng DC. Iron Sucrose Accelerates Early Atherogenesis by Increasing Superoxide Production and Upregulating Adhesion Molecules in CKD: *Journal of the American Society of Nephrolody (JASN).* 2014; 25 (11):2596-2606.

27. Oliveira MC, Coutinho LB, Almeida MPO, Briceño MP, Araujo ECB, Silva NM. The availability of iron is involved in the murine experimental Toxoplasma gondii infection outcome. *Microorganisms.* 2020; 8(4): 560.

28. Paget GE, Barnes JM. Evaluation of results: Qualitative application in different species. In: Laurence DR, Backarach AL (eds.), Evaluation of drug activities. Pharmacometrics. *Academic press, London and New York.* 1964; 491(4):4691.

29. Kiernan JA. Butterworth-Heinemann (Reprinted 2000; London: Arnold Publishers). Histological and Histochemical Methods*: Theory and Practice*; 1999.

30. Elgendy DI, Othman AA, Saad MH, Soliman NA, Mwafy SE. Resveratrol reduces oxidative damage and inflammation in mice infected with Trichinella spiralis. *Journal of helminthology.* 2020; 94:140.

31. Conn J. Biological Stains, 9th ed., Baltimore: Williams and Wilkins Co; 1977.

32. Wilcock D, Gordon M, Morgan D. Quantification of cerebral amyloid angiopathy and parenchymal amyloid plaques with Congo red histochemical stain. *Nat Protoc 1*. 2006; 1591–1595.

33. Skariah S, McIntyre MK, Mordue DG. Toxoplasma gondii: determinants of tachyzoite to bradyzoite conversion. Parasitology research. 2010 Jul;107:253-60.

34. Eissa S, Shoman S. "Markers of invasion and metastasis and markers of tumor proliferation and apoptosis. *Tumors markers.* 1998; 131-153.

35. Rishi G, Subramaniam VN. The liver in regulation of iron homeostasis. Am. J. Physiol. Gastrointest. *Liver Physiol*. 2017; 313: 157–165.

36. Arroyo R, Ochoa T, Tai JH, de la Garza M. Iron and parasites. *BioMed Research Internationa*l. 2015; 2015: 291672.

37. Aghabi D, Sloan M, Gill G, Hartmann E, Antipova O, Dou Z, Guerra AJ, Carruthers VB, Harding CR. The vacuolar iron transporter mediates iron detoxification in Toxoplasma gondii. *Nat Commun.* 2023 Jun 20; 14(1):3659.

38. He JJ, Ma J, Elsheikha HM, Song HQ, Huang SY, Zhu XQ. Transcriptomic analysis of mouse liver reveals a potential hepato-enteric pathogenic mechanism in acute Toxoplasma gondii infection. *Parasites & vectors.* 2016**;** 9(1): 1-13.

39. Alvarado-Esquivel C, Torres-Berumen JL, Estrada-Martínez S, Liesenfeld O, Mercado-Suarez MF. *Toxoplasma gondii* infection and liver disease: a case-control study in a northern Mexican population. *Parasit Vectors.* 2011; 4:75.

40. Dziadek B, Dziadek J, Dlugonska H. Identification of Toxoplasma gondii proteins binding human lactoferrin: a new aspect of

rhoptry proteins function. *Experimental parasitology*. 2007; 115(3), 277-282.

41. Blader IJ, Manger ID, Boothroyd JC. Microarray analysis reveals previously unknown changes inToxoplasma gondii-infected human cells. *J Biol Chem.* 2001; 276: 24223–24231.
42. Dimier IH, Bout DT. Interferon-gamma-activated primary enterocytes inhibit Toxoplasma gondii replication: a role for intracellular iron. *Immunology.* 1998; 94(4):488-495.
43. Almeida MPO, Ferro E.AV, Briceño MPP, Oliveira MC, Barbosa BF, Silva NM. Susceptibility of human villous (BeWo) and extravillous (HTR-8/SVneo) trophoblast cells to Toxoplasma gondii infection is modulated by intracellular iron availability. *Parasitology research.* 2019; 118(5): 1559-1572.
44. Becerril-Ortega J, Bordji K, Fréret T, Rush T, Buisson A. Iron overload accelerates neuronal amyloid-β production and cognitive impairment in transgenic mice model of Alzheimer's disease. *Neurobiology of aging.* 2014; 35(10), 2288-2301.
45. Belaidi AA, Gunn AP, Wong BX, Ayton S, Appukuttan AT, Roberts BR, Duce JA, Bush AI. Marked age-related changes in brain iron homeostasis in amyloid protein precursor knockout mice. Neurotherapeutics. 2018 Oct 14;15:1055-62.
46. Liu B, Moloney A, Meehan S, Morris K, Thomas SE, Serpell LC, Hider R, Marciniak SJ, Lomas DA, Crowther DC. Iron promotes the toxicity of amyloid β peptide by impeding its ordered aggregation. Journal of Biological Chemistry. 2011 Feb 11;286(6):4248-56.
47. Beaman M, Remington J. Cytokines and resistance against Toxoplasma gondii: evidence from in vivo and in vitro studies. . *The Biomedical Press.* 1992; 111-119.
48. Beaman M, Hunter C, Remington J. Enhancement of intracellular replication of T.gondii by IL-6. Interaction with IFN-γ and TNF-α. *J Immunol.* 1994; 153: 4583-4587.
49. Nemeth E, Tuttle MS, Powelson J, Vaughn MB, Donovan A, Ward DM, et al. Hepcidin regulates cellular iron efflux by binding to ferroportin and inducing its internalization. *Science*. 2004; 306: 2090–2093.
50. Misumi S, Kim TS, Jung CG, Masuda T, Urakawa S, Isobe Y, Hida H. Enhanced neurogenesis from neural progenitor cells with G1/Sphase cell cycle arrest is mediated by transforming growth factor β1. *European Journal of Neuroscience.* 2008; 28(6): 1049-1059.
51. Qayoom A, Aneesha VA, Anagha S, Dar JA, Kumar P, Kumar, D. Lecithin-based deferoxamine nanoparticles accelerated cutaneous wound healing in diabetic rats. *European Journal of Pharmacology*. 2019; 858: 172478.
52. Mostafa E, Ahmed FA, Yahia SH, Ibrahim AI, Elbahaie ES. The effects of intracellular iron availability on the outcome of Toxoplasma gondii infection in mice. *Journal of Parasitic Diseases.* 2023; 13:1-1.
53. Massague J. TGF beta signalling in context. *Nat Rev Mol Cell Biol.* 2012; 13(10):616–630.

Cite as: Mostafa, E., Abdel-Hameed, B., Yousef, A. The Outcome of Therapeutic Trials Using Iron and Iron Chelator in Acute Murine Toxoplasmosis: Histopathological and Immunohistochemical study. *Afro-Egyptian Journal of Infectious and Endemic Diseases*, 2024; 14(2): 214-226. doi: 10.21608/aeji.2024.272563.1360